

We are IntechOpen, the world's leading publisher of Open Access books Built by scientists, for scientists

6,100

Open access books available

149,000

International authors and editors

185M

Downloads

Our authors are among the

154

Countries delivered to

TOP 1%

most cited scientists

12.2%

Contributors from top 500 universities



WEB OF SCIENCE™

Selection of our books indexed in the Book Citation Index
in Web of Science™ Core Collection (BKCI)

Interested in publishing with us?
Contact book.department@intechopen.com

Numbers displayed above are based on latest data collected.
For more information visit www.intechopen.com



Characterization of Macro- and Micro-Geomorphology of Cave Channel from High-Resolution 3D Laser Scanning Survey: Case Study of Gomantong Cave in Sabah, Malaysia

Mohammed Oludare Idrees and Biswajeet Pradhan

Additional information is available at the end of the chapter

<http://dx.doi.org/10.5772/intechopen.69084>

Abstract

Three-dimensional documentation of hypogene cave morphology is one of the major applications of laser scanning survey. This chapter presents applications of terrestrial laser scanning (TLS) survey for analyzing endogenic cave passage geomorphologic structure and morphometry using 3D meshing, high-resolution 3D texture modeling for geovisualization, and its potential for cave art documentation. To achieve this, multi-scale resolution 3D models were generated; one using the mesh model for macro-morphological analysis and the other with the full-resolution scan to produce high quality 3D texture model for identification of micro-morphological features. The mesh model of the cave makes it possible to analyze the general shape, distinguish phreatic tube from post-speleogenetic modified conduits and carry out morphometric measurements including the cave volume and channel surface area. The 3D texture model provides true to live visualization of the cave with exceptionally high level of accuracy and details that would be impossible to obtain with direct observation by visiting the site or from the mesh model. The model allows discerning different speleogenetic phases, karstification processes and micro-morphologies such as wall and ceiling seepage, hanging rocks, fractures, scallops, ceiling flush dome, pockets, bell-hole and avens. Also, the texture model permits identifying cave arts and engravings along the passages

Keywords: virtual geomorphology, texture model, cave, passage failure, terrestrial laser scanning, Gomantong cave

1. Introduction

Caves are natural resources of complex dimensions that require intelligent planning and management for sustainability. They are naturally formed caverns that have played diverse roles for the human and animal communities. Investigations have revealed primordial use of caves on a short- or long-term basis depending on the nature of activities they are used for or the circumstances that necessitate the usage [1]. Caves have been used by man as shelter and for protection during wars. In many cultures, people bury their dead ones in caves occasionally, with their belongings and gift to help them in their spiritual journey. Man has used and continued to use caves for ritual and religious functions till this present time. Studies have also confirmed that caves were used for industrial purposes. For example, relict ceramic and metal deposits found in the French Bronze Age cave, Les Fraux, indicate that the ancient bronze workers used the cave as “industrial” workshop [2]. It is also on record that Bedeilhac cave, in the French Pyrenees, was used as aircraft factory during the post-Industrial Revolution [1].

Human beings are rarely the first to explore caves. Caves are favourite natural habitat for varieties of animals, such as pigs, primates, elephants, hornbills, bats, birds, reptiles, amphibians and other organisms, some of which are endangered. Evidence of visitation of animals to some caves has been found in their dung and bones. For example, skeleton of a young elephant was found in a cave in Pahang, Malaysia [3]. Likewise in Kitum caves, Kenya [3] reported the regular visits of elephants to eat minerals from the rocks. For over 600 years, the Great Niah and Gomantong caves in Sarawak and Sabah, Malaysia Borneo, have been famous for sheltering large colonies of bats and swiftlet birds [4].

This age-long interaction of man and animals in caves has resulted in enormous treasures within the confinement of the environment, albeit, it has also endangered the delicate cave ecosystem. In the interest of exploration, exploitation and preservation of the cave environment, man has devised several methods of surveying cave and tracking the resources therein in line with advances in technology of surveying instrumentation. Historically, earliest cave explorers used sketches to communicate or report their observations and findings in the cave. As time passed by, traditional instruments such as compass, clinometers and theodolites progressively became handy for cave mapping. By the turn of 1961, light amplification by stimulated emission of radiation (laser) began appearing on commercial markets for medical application and ranging. Subsequently, rangefinder and total station emerged with laser-ranging capability, collecting single-point $xy(z)$ data at a time. Then, cave mapping became much easier and accurate than with compass and inclinometer; however, cave maps were still delivered in 2D space.

Today, sophisticated light-scanning (or laser-scanning) sensors that are capable of collecting several thousands to million points per seconds have taken over from the traditional methods, delivering caves in their true 3D geometry at unprecedented level of accuracy [5]. Terrestrial laser scanning (TLS) survey has proven positive results in different applications

such as archaeological investigations, 3D modelling and visualization, geomorphological analysis, passage stability and risk assessment, biological inventory and so on. A comprehensive review of the journey of laser scanning to caves including method, progress in hardware and software development for data collection and processing can be found in Ref. [6].

Awareness of the wealth of information conveyed in laser-scanning data and the significant role high-resolution 3D documentation can play in deepening the complete understanding of the cave motivates this present investigation. We propose that 3D texture model can offer an excellent platform for geomorphological investigations with high level of accuracy through virtual cave tour. So, building on the foundation of Ref. [7], this study experiments virtual geomorphological analysis with laser-scanning data collected in the less-accessible Simud Putih. The aim is to generate multi-scale resolution 3D models. One, using the 3D mesh model for macro-morphological analysis and the other, with the full-resolution scan to produce texture model for identification of micro-morphological features. The investigation revolves around three applications with the following objectives:

- Modelling the cave in 3D space at different resolution scales for analysing endogenic passage geomorphologic structure and morphometry.
- Identification of micro-geomorphological features of the floor, wall and roof through virtual cave exploration with high-resolution 3D texture model and its potential for cave art documentation.

On this note, this chapter on “Characterization of macro and micro-geomorphology of cave channel from high-resolution 3D laser scanning survey: a case study of Gomantong cave, Sabah (Malaysia)” presents the approach employed for the multi-scale resolution 3D modelling of Simud Putih and the different applications they were used for. The structure of the chapter is organized thus: following this introduction, the second part describes the location of the cave with emphasis on the geographic location, geology and speleogenesis. In the third part, the general methodology with terrestrial laser scanning, including (i) planning, (ii) 3D laser scanning survey and (iii) point cloud processing, is sequentially articulated. Other specific data-processing tasks for the target applications will be done within the context of the individual subsection. The fourth part outlines and discusses the results of the case study and their applications. The last part is the concluding remarks and the future research outlook.

2. Geological setting and study area

Geographically, Gomantong cave is located in a tower-like limestone outcrop that projects approximately 300 m above a floodplain on longitude 118° 04' E and latitude 5°32' N within the Sabah forest reserve [7]. Travelling by road, the hill lies some 31.4 km south of Sandakan and about the same distance to the east of Kota Kinabatangan, the state capital of Sabah, Malaysia (**Figure 1**).

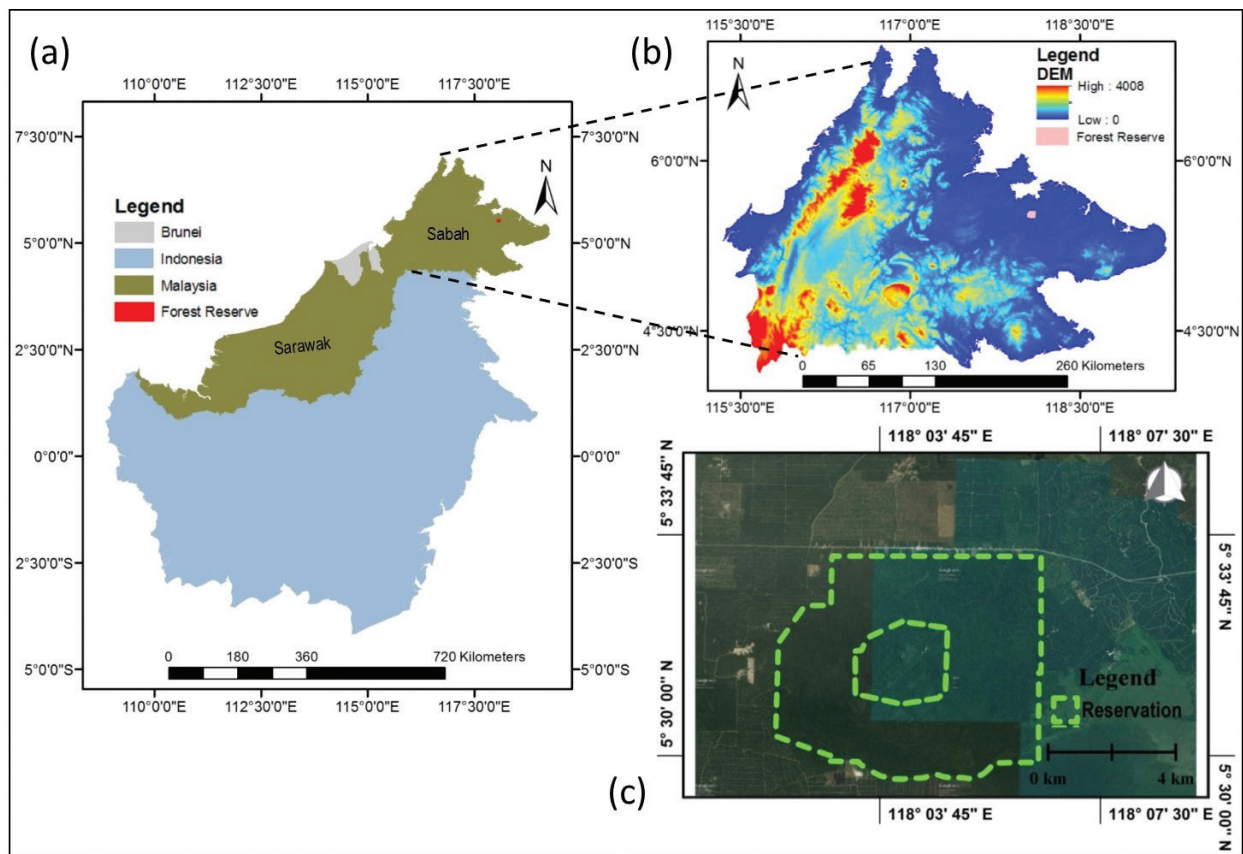


Figure 1. Location of Gomantong cave in (a) Borneo Island, (b) ASTER-GDEM of the state of Sabah (Malaysia Borneo) and (c) Google Earth image of Gomantong forest reserve with the hill at the centre.

From geological point of view, the limestone contains dense lithic fragments of grey sedimentary rock rich in organic matters deposited in laterally thin and well-defined layers that lie uncomfortably on the underlying Labang bedrock [8]. The layers alternate with bed of thin grey-green fossil and sometimes intercalated by sandstones and shales of the Oligocene Labang formation. Evidence from nanofossil dating of samples taken from marls, mudstones and on benthic foraminifera across the region estimates the formation age at about 23 million years ago—between late Oligocene and early Miocene [8, 9]. The detritus particles are believed to have recrystallized during the Oligocene sediment formation, resulting in varying sizes of the crystal structure in the uplifted rock.

In terms of speleogenesis, the cave is believed to have started immediately after the uplift, compression and folding of the rock during the early Pliocene which was followed by dissolution of soluble rocks along bedding planes and joints [7, 9]. Gomantong cave system consists of two major passages, one above the other [10]. The lower cave, locally referred to as Simud Hitam, provides entrance along one of the major faults that opens to the base of the hill and coincides with the ground level of the bank of a small stream nearby. But, for the upper level cave (Simud Putih), the access is situated some 85 m above the floor of the opening to the lower cave [10].

Like every other cave, this one is dark and humid, providing an excellent microclimate habitat that is suitable for swiftlet birds and bats in their millions to share [11, 12]. In addition, the

cave provides naturally confined speleogenetic setting that makes it particularly attractive. Swiftlet birds and bats contribute significantly to ecosystem engineering, tourism and economy of the state of Sabah [13]. However, there are indications of threat of potential collapse of the cave due to natural and anthropogenic causes [7].

The danger posed by over-exploitation to the survival of the Gomantong cave system requires holistic approach to confront the multifaceted challenges resulting from the activities of man, animals and nature combined. For example, the cave passage of Simud Hitam has been extremely affected by biogenic corrosion. Equally, the cave wall and roof are frequently hacked to provide support for hanging ladders through which edible nests are reached. All these, in addition to natural geologic processes, weaken the structure and thereby accelerate the rate of deformation in the cave. Since the last six centuries, the cave has been one of the focal references to edible bird-nest (EBN) harvesting in southeast Asia [7]. While the business flourishes, enriching the economy of the state and her indigenous residents, the survival of the cave itself for life-long production of this lucrative commodity has been largely neglected, though unintentionally [4], despite the vicious impact of biologically induced alteration of the cave passage. In this regard, provision of adequate information about the internal structure of the cave will be of paramount assistance to decision makers and cave managers on the best way to protect the cave and its resources.

Recent investigations by Refs. [7, 10] show that little is known about the cave structure, and particularly the geomorphology, thereby throwing an open challenge to the research community on the urgent need for deeper exploration. Nevertheless, stakeholders were sufficiently alerted on the danger of continuous deformation of the cave cavity should biogenic decay persist [7]. However, the message could not be clearly conveyed with respect to the cave geometry to the stakeholders who, mostly, are non-technical professionals. The reason being that the data were collected using traditional survey method, and the information presented in 2D, making it impossible to visualize the enormity of the biogenic activities in the cave.

Another concern is that the foregoing investigation was carried out in Simuh Hitam (lower cave), near the entrance where daylight penetrates to illuminate the cave. Thus, the internal geomorphology including the ongoing deformations of the cave cannot be described. Moreover, the distance of the cave roof from the floor is far and barely visible to an observer from the latter. The second study [10] utilized 3D scanning; nonetheless, only the basic quantitative measurements (length, area and volume) were extracted. The lower cave has always been given more priority in terms of research mainly because of its ease of access. This accounts for why most of the studies about the cave system have focussed on the lower section while the upper cave chamber has not been widely explored. For that, this present study centres entirely on the upper cave.

3. Materials and method

The overall methodological workflow used in this study is presented in **Figure 2**.

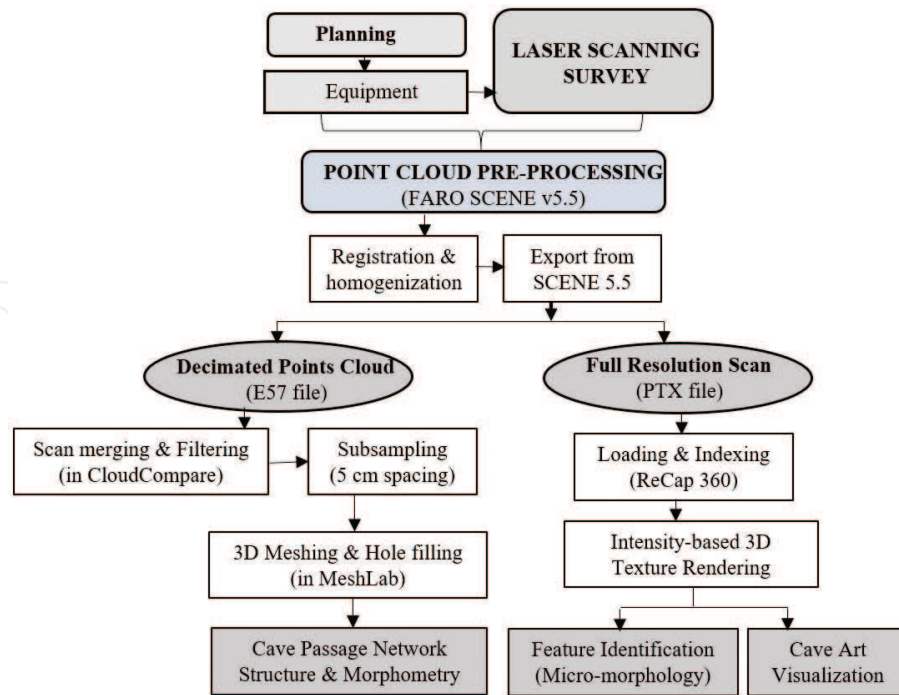


Figure 2. Data processing and analysis workflow.

3.1. Terrestrial laser scanning survey

The procedure presented here follows the established workflow for point data collection and processing: planning, field work and point cloud processing [6]. In July 2014, FARO Focus3D was used to scan Simud Putih to complement the 2012 scanning expedition in Simud Hitam [14]. The scanner employs the phase-shift scanning technology with exceptional distance accuracy up to a scanning range of 120 m. Like every other scanner, Focus3D measures distance to a target by comparing the difference in pulses of emitted and reflected wavelengths. The use of this particular scanner was evaluated on the basis of its technical suitability (**Table 1**). In the market today, Focus3D is the lightest and smallest high-speed scanner designed for outdoor and indoor applications [6]. The size and weight (~5 kg) of Focus3D, high accuracy, rapid rate of data collection and extended battery life of 4.5 h make it a suitable choice for high-precision survey in caves.

Planning is necessary to increase the efficiency of data collection and processing manoeuvres for high-quality point cloud and 3D reconstruction [15]. Therefore, ahead of the field work, the cave was visited during which scanning positions were strategically predetermined to achieve good overlapping areas. Sufficient overlap between adjacent scans increases the quality of registration process and also provides complete data coverage. Moreover, distance between scanning positions and between the cave wall and the instrument was kept roughly at regular intervals to ensure consistent scan resolution.

During the data collection, a total number of eight spherical targets were used to support scan registration process. The targets were placed around the scanner field of view such that at least three or more can be visible in two adjacent scans for high-quality registration. Where

Feature	Specification
Manufacturer	FARO
Model	FARO Focus ^{3D}
Range	0.6–120 m indoor or outdoor with low ambient light and normal incidence to a 90% reflective surface
Ranging error ²	±2 mm
Measurement speed	122,000/244,000/488,000/976,000 points/s
Field of view	Vertical/horizontal: 305/360°
Weight	5.0 kg
Size	240 × 200 × 100 mm ³

Table 1. Technical specifications of FARO Focus3D terrestrial laser scanner.

reference to national or global coordinate system is required, the target positions are measured accurately using theodolite, total station or a combination of GPS and total station [16, 17]. Advances in hardware and software development have provided alternative scan registration procedures such as cloud-to-cloud and automated registration in target-less mode. Nevertheless, the need for target-based scan matching cannot be overlooked particularly in cave interior that is characterized by irregular formation, difficult access and unfavourable working environment. On each station, scanning was done at one-fourth scan resolution mode which provides 244,000 points/seconds and x-y point cloud spacing of 12.5 ± 2 -mm ranging error at a distance of 20 m [14]. Overall, a total number of 203 scans were collected during the two weeks' field work that resulted in over 6.09 billion points of ~38.0 GB. Out of 203 scans, only 99 scans that represent the main passages of the upper-level cave were further processed and used for this study.

3.2. Point cloud processing

Since the scans were collected from different positions, it was necessary to align the individual scan into one set of point cloud. This was done using the proprietary SCENE-5.5 software (www2.faro.com/downloads/training/Software). For high-quality registration, semi-automatic target-based point correspondence utilizing the reference sphere placed within scan areas was used. The method employs the iterative closest point (ICP) [18] algorithm which automatically detects at least three artificial target points that are visible in successive adjacent scans to compute accurate transformation parameters. The process was further improved by activating auxiliary sensors (inclinometer, compass and altimeter) to speed up the correlation of the individual scans. The emerging trend in the new generation of scanners such as Focus3D x330, x130 and Z+F Imager 5010X is the evolution of multi-sensor scanning hardware including GPS receivers, inclinometers, inertial measurement unit (IMU), compass, powerful imaging cameras and height compensator that enhances the quality and accuracy of data collection and processing.

This particular study does not require reference to national or global coordinate system; hence, the scanner's local Cartesian system was sufficient. Usually, the first scan station

is taken as the origin where the instrument's plumb line provides the z-axis [15], and the horizontal line is defined by the scanner's internal compass which facilitates aligning scans to geographic direction. The registration quality produced root mean square error of 0.0044 RMSE, equivalent to 4.4 mm. The registered point clouds were exported from SCENE software as an individual file in ASTM E57 file format for 3D imaging data exchange [19] and PTX file format, respectively. The E57 file format offers efficient storage and data compression that facilitates ease of 3D data transfer across different platforms better than ASCII-based point cloud exchange format like PTX. PTX file preserves all of the information from the original scan (scanner location) plus additional registration information (transformation matrices). The drawback of PTX is that it requires large memory space to keep the information. The aligned scan yielded point spacing of < 6 mm in both the horizontal and vertical axis.

For 3D reconstruction and rock structural analysis, processing the full-resolution scan is not computationally efficient [5]. Therefore, the E57 format point cloud dedicated for these applications was decimated by sampling every seventh point to optimize processing time based on the suggestion of Ref. [5]. In CloudCompare [20], a free and open source software, the decimated scans were merged to provide a single discontinuous point cloud of the cave. Thereafter, the matched point cloud was filtered to eliminate noise, while other points belonging to features outside the cave were manually deleted. Finally, the cleaned point cloud was spatially sub-sampled using horizontal and vertical distance spacing of 5 cm between points for efficient mesh generation. Further, application-based data processing and analysis using either the decimated or full-resolution scan point cloud are discussed in section 3.3.

3.3. Application-specific data processing

3.3.1. 3D Meshing and passage geomorphology

The sub-sampled point cloud in Section 3.2 was used for the 3D surface reconstruction. Point cloud comprises a set of dense 3D xyz points of the surface, but, in reality, the discrete point data do not offer sufficient description of the cave structure. 3D mesh generation was done in MeshLab 1.3.4BETA [21] to reconstruct the cave in its true 3D geometry. MeshLab is an open source package for point cloud processing, advance mesh generation and editing. A number of surface reconstruction approaches are available in the software but the widely used Poisson surface reconstruction approach was applied in this present chapter. The algorithm utilizes the sampled points from the surface and the gradient of the indicator function (a normal field) to build surface. The gradient of indicator function was derived by computing normals for the point sets using 10-point neighbourhood kernel. The procedure converts the point normal into a solid 3D surface by defining a scalar function that best matches the vector field to build a fitting isosurface [22, 23]. The 3D meshed surface was achieved with octree depth of 10 comprising 825,451 vertices and 1,650,604 faces. Octree depth parameter sets the depth of the octree used for extracting the final surface. Increasing the octree depth parameter increases the precision and level of details (faces and vertices) of the surface; however, compromise had to be made among level of details, visual reality and real-time interaction with the model. The final mesh model was used for analysing the general cave passage structural morphology and morphometry and also for the sectional drawing.

3.3.2. Textured 3D modelling for detail micro-morphologic and cave art identification

Documenting micro-morphological features requires high-resolution textured 3D model. Advances in computational efficiency of point cloud processing software like Autodesk ReCap and its textural 3D rendering capability will rapidly revolutionize cave investigation. Despite the tremendous success achieved with TLS survey in many notable caves around the world, photo-realistic 3D rendering of cave has remained unattainable. Besides the limitation of the existing point cloud processing software in handling large volume of data, overcoming the problem of total darkness has been a subject of intensive research [24–27]. Today, archaeological documentation using 3D scanning is considered the best method; nevertheless, the use of two independent sensors, laser scanning and digital photos throws up additional challenge. The difficulties include managing illumination variation, finding exact match between the images and geometric model and handling the volume of data acquired [27]. Besides, processing the data involves several manual operations.

As an alternative approach to RGB (red, blue and green) photos, the laser intensity value attached to each point was used as a substitute for the texture-based virtual reality rendering. In this study, we used Autodesk ReCap360 student licence package (<http://www.autodesk.com>) [28]. ReCap360 is one of the families of Autodesk products specifically designed for handling massive cloud point and photo dataset. It is innovative 3D modelling and reality capture software that create complex 3D model with real-world visualization by combining laser scans and photos. The package supports a number 3D file formats including CL3 (Topcon), E57, FLS (Faro), LAS, PCG, PTG (Leica), PTS, PTX, RCS, TXT, XYZ and ZFS (Zoller+Fröhlich). Moreover, it computationally optimizes input files by indexing to its native RCP file format for efficient processing, modelling and interactive visualization. The model allows complete natural feel of the rock such that all details of the irregular surfaces including rock engraving and artworks in their true 3D geometry are captured.

Understanding cave use, especially in the past, requires detailed true-to-life perception of the space in all dimensions including the morphogenesis of the floor, ceiling and wall caused by geological and, at times, biological factors. For Gomantong cave, no reference is found in the literature indicating cultural utilization of the subterranean space in the past outside nest harvesting. This aspect of our study aims at identifying micro-morphologic features and relict antiquity from the high-resolution 3D texture model that could provide insight into factors that influenced passage modification and enhances our knowledge of probable age-long use of the cave.

4. Discussion

4.1. Cave passage network structure

One of the main objectives of this study is to provide interactive digital representation that permits visualizing the entire cave network morphology in 3D space, and also, to allow extraction of features in their geometrically correct dimension without visiting the cave. The dipping limestone produced a particular style of cave that can only be comprehended

in digital model. Meshing produced cave surface that provides exact representation of the arrangement, structure and irregularities (**Figure 3**). The cavity comprises connected passages geographically oriented to different directions. For specific description of cave channels and their morphological characteristics, the passages are classified into six segments (entry, chamber, hall and shafts 1, 2 and 3) according to their global orientation.

Meshing provides the structural construct of the pattern of the cave network. Externally, the plan view of the cave (**Figure 3b**) presents a system of network connectivity that bears a resemblance to typical Uzi Galil sniper rifle with each component (handle, butt, trunk, magazine and precision telescope) forming different channels, for example, entry passage, chamber, main hall, shafts 1 and 2 and shaft 3 in that order. The primary passage to the main hall starts off vertically downward to about 29 m at a very steep slope and then trends east-west, parallel to the main chamber, to join the hall. The chamber also connects the main hall at the upper-most end in the northern side through an orifice that dips west-east. This main hall is a large cavern that runs NE-SW, connecting the SE-NW trending shafts (1 and 2) and the inclined N-S shaft 3 (**Figure 3**).

The model allows cave interior visualization at the coarse level, while also permitting the extraction of dimensional data with detailed geometric definition and precise graphic description of the cavities (**Figure 4**). 3D mesh gives a feel of the general complex morphogenetic

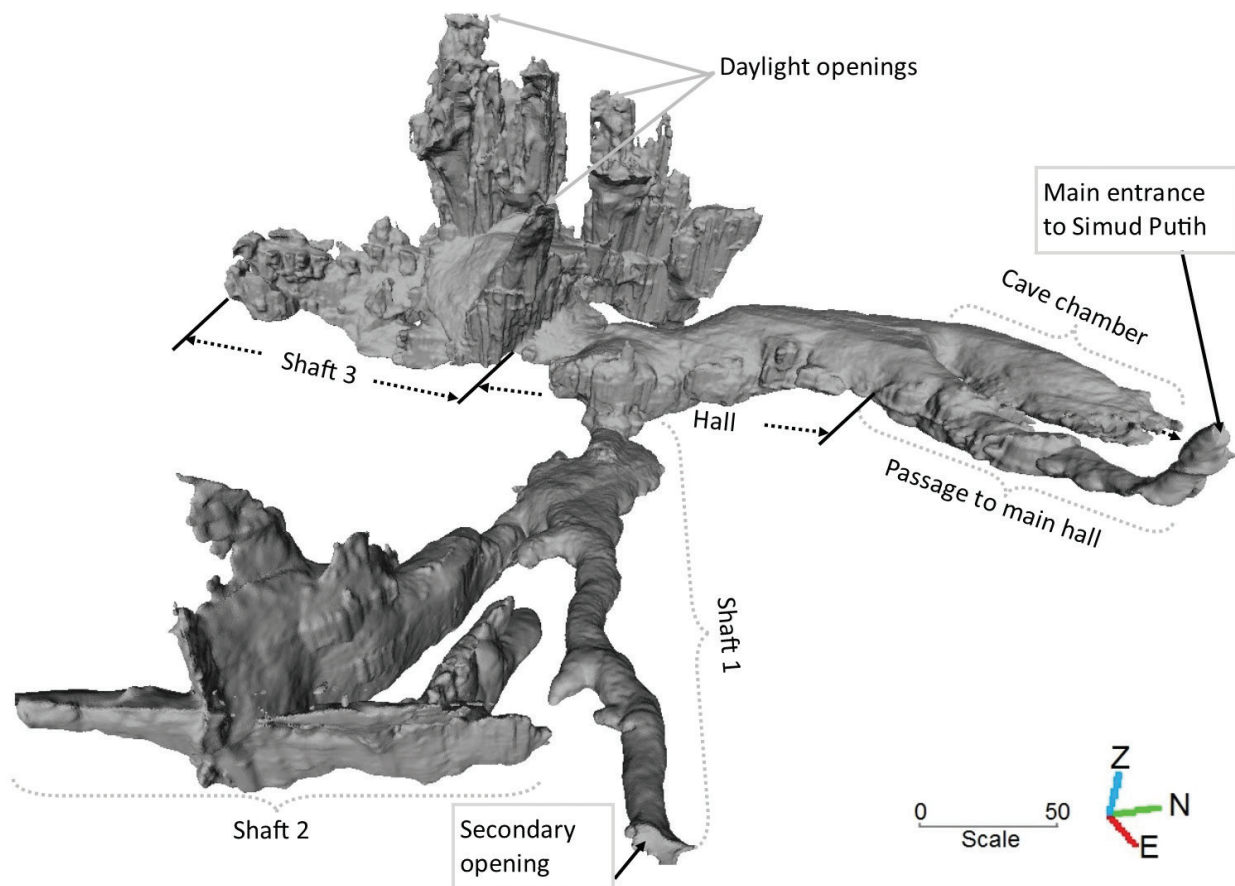


Figure 3. 3D model of the upper level cave (Simud Putih) produced in MeshLab with ≈ 28.3 million points at an octree depth of 10.

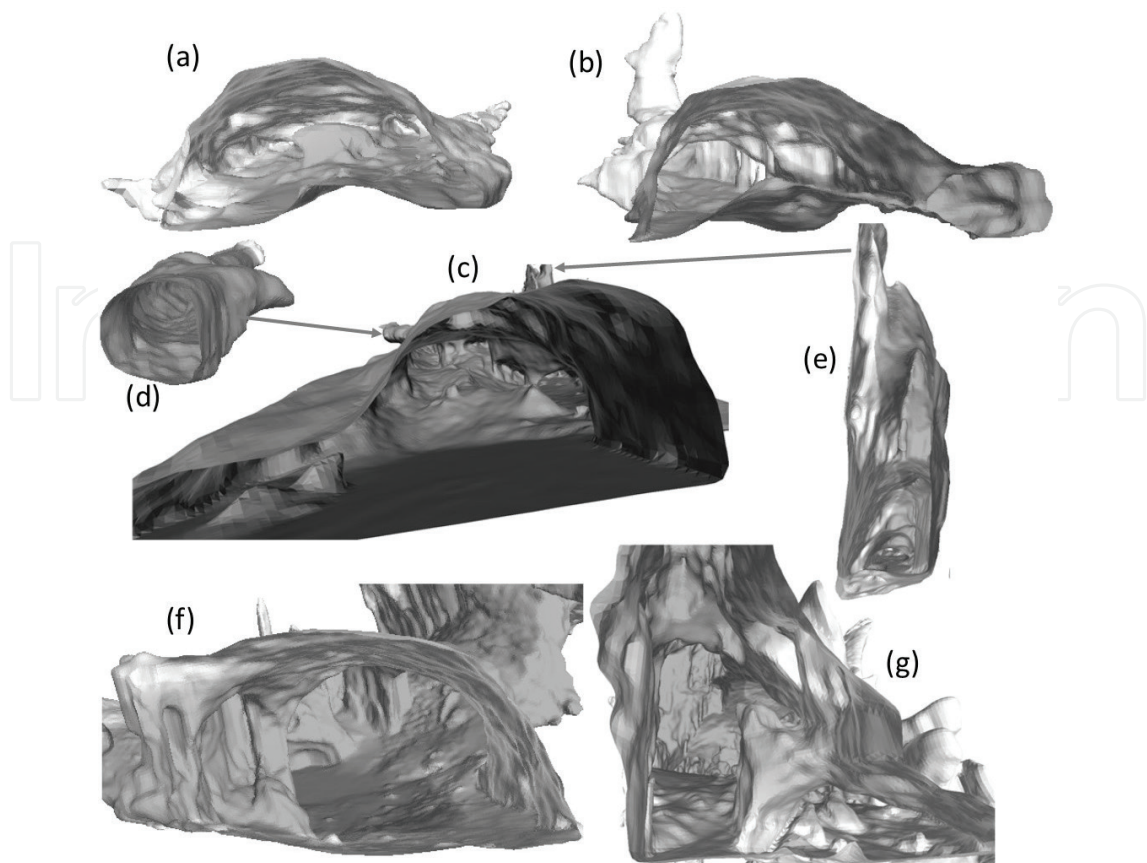


Figure 4. Graphic description of the cave cavities: (a) main chamber viewed W-E, (b) the horn-shaped entry passage viewed W-E, (c) secondary chamber where shaft 1 (d) and shaft 2 (e) are connected, (f) main hall viewed from N-E to S-W at the centre of the hall and (g) shaft 3 viewed towards the north direction.

characteristics of the karstic landform. Precisely, the model shows that the passages mostly still retain their original phreatic tube except for shaft 3 and the burgeoning section of shaft 2. Although there is no active stream flowing in it, there is evidence of flooding during heavy precipitation particularly within the secondary chamber that connects shafts 1 and 2 to the terminal section of the hall which forms the lowest elevation of the cave. The floor also appears more solidly intact except with some isolated rock piles but is a relatively gentle undulating surface of interchanging concave and convex arc that cambers to each side creating shallow erosional bench at the edges (Figure 4a–4c and 4f). Figure 5e and 5g depicts roof patterns that may have originated from lateral strike slip and fault-controlled attritions. The wall largely comprises tri-oval conduit arm, buttress, vertical and semi-circular walls holding the dome roof.

4.2. Cave morphometry

An overview of the shape characteristics of each segment is shown in Figure 5. The sectional drawing improves the understanding of the internal outline of conduits at the roof and floor sections. It can be seen that the cave passages vary in height and width, which implies that the cavities either respond differently to denudation or are developed across different timelines. The shapes of the passages vary from simple flute morphologies to rather complex features with overhang, pillars, horn-like extension and step-tile cathedral interior formations (Figure 5).

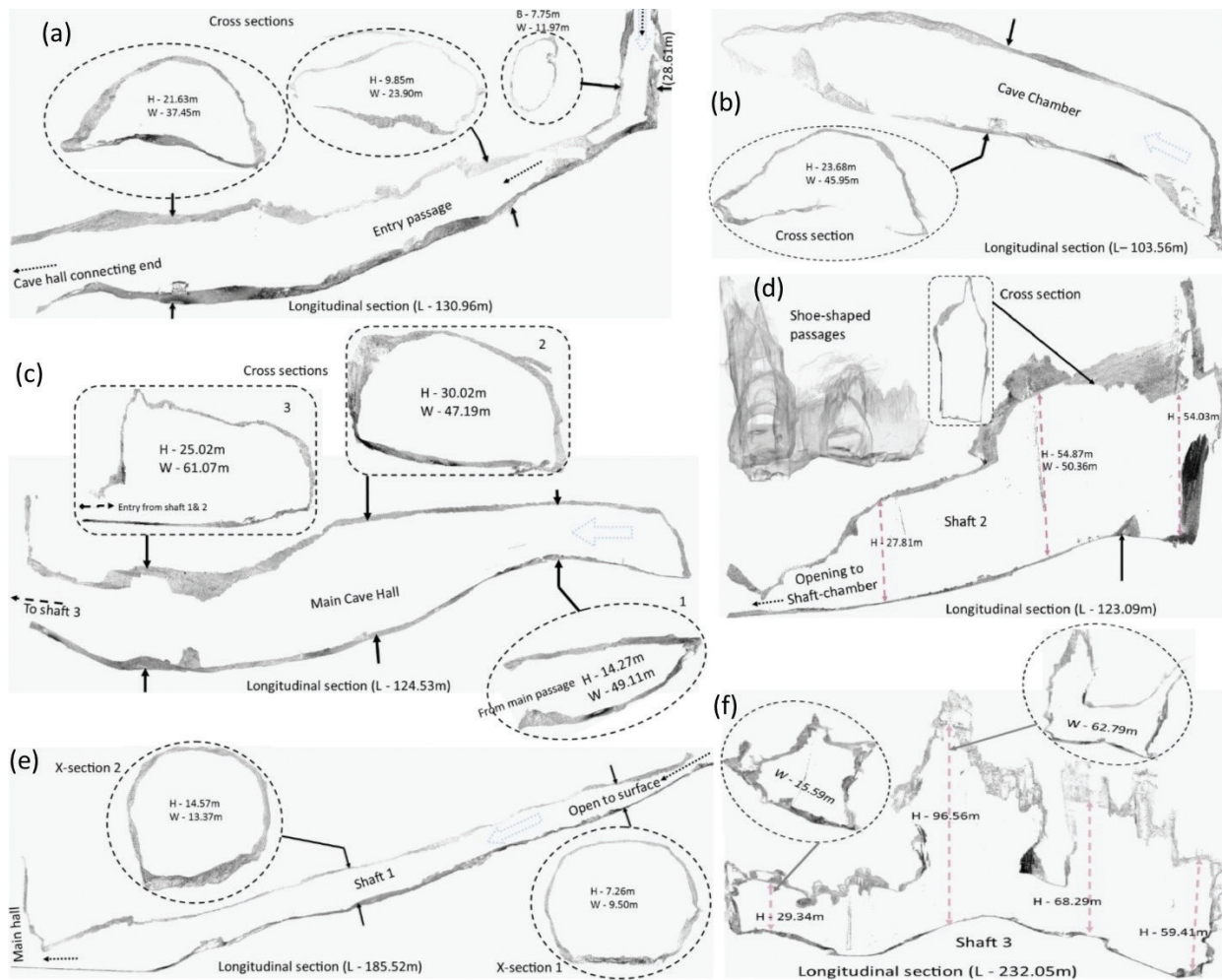


Figure 5. Side and cross-sectional view highlighting passage outline of (a) entry channel, (b) chamber, (c) main hall, (d) shaft 2, (e) shaft 1 and (f) shaft 3.

Dimensionally, the cave extends linearly from sub-metre openings to impressive passage width of up to 65 m, varying heights and several metres' penetration depth developed along major tectonic features like faults, fold cores and bedding contact. All the passages descend to the more distant part to converge at a central area down south of the main hall that forms the lowest part of the cave network. The floor at this minimum elevation is relatively flat (**Figure 5c** and **5e**) and filled with sediments, pebbles and flowstone. The impact and degree of weathering activities are more pronounced at the cave ceiling with exciting irregular shapes that provoke closer examination particularly in shafts 2 and 3. In general, the mesh model facilitates quantitative measure with better accuracy (**Table 2**).

The entrance to the cave is located in vertical rock walls of about 29-m depth from the top of hill and continues deeper along a steep rock wall down the hillslope to the main hall (**Figure 5a**). The cavity becomes wider as it advances towards the hall, forming a horn-shaped hollow and terrace outline at the roof. Entry passage and chamber connect the large lofty hall that constitutes the primary trunk of the cave system. The chamber (**Figure 5b**) has a high-domed formation that looks like the hard-upper shell of tortoise (carapace) but at the base, a

Total length (m)	1,043.05
Total floor area (m ²)	38,575.00
Passage surface area (m ²)	155,414.00
Passage volume (m ³)	735,226.00

Table 2. Summary of basic geometric properties of the model.

convex silhouette slopes to the foot of the wall at both sides. The hall has a rectangular shape of about 50–70-m width, a buggy-top roof of up to 30-m height and a basin morphology landform at the floor (**Figure 5c**).

Passage layout of shaft 1 (**Figure 5e**) is unique; the conduit forms a long tubular flute-shape passage with oval outline in cross section along the entire length of the strait. Like the entry passage, the conduit has erosional contact with the surface but at a relatively gentle gradient that allows a steady slipping down of rainwater and eroded materials along the slope. It is probably the youngest passage because it exhibits undisturbed early stage phreatic tube formation with scallops freshly sculptured in the roof and wall of the tube.

In contrast, shafts 2 and 3 show completely different morphologies especially at the roof. The former is a boot-shaped twine passage lying 30-m apart and is linked by a narrow vertical channel of approximately 42-m height (**Figure 5d**). The right passage which is about 60-m long terminates at a dead end while the other “leg” extends to about 123 m and joins a small chamber through a narrow opening that connects it with shaft 1. The two have similar morphologies that take the shape of a wellington boot. Shaft 3 (**Figure 5f**) produces a typical cathedral morphology with step-tiles roof. The interior has been severely weathered, thus creating different karstic formations including enormous cavern resulting from breakdown chamber, multi-storey passages, avens and epikarstic seepage.

As a conclusion, the mesh model provides adequate information to describe the general cave network, internally and externally, which has never been done. Furthermore, we were able to produce the cross section and obtain accurate morphometrics of the model (**Table 2**). However, the coarse nature of the source point cloud and lack of texture information limit the amount of details that can be extracted from the model.

4.3. Identification of micro-morphological features

Intensity-based texture model shows all the fine geometric details that bring true-to-life virtual caving with complete representation of the interior “infrastructure” (**Figure 6**). In contrast to the mesh model, the texture model reveals all the signs of epigenetic speleogenesis in addition to identification of fine detailed morphological features. Apart from these, dimensional measurements of sub-millimetre accuracy can be obtained. Certainly, the challenge of visualizing cave interiors due to lack of illumination is solved with this approach.

Generally, it can be noticed from the texture model that all the passages, except shafts 2 and 3, have scallops on their wall and roof, indicating the extent to which the original phreatic

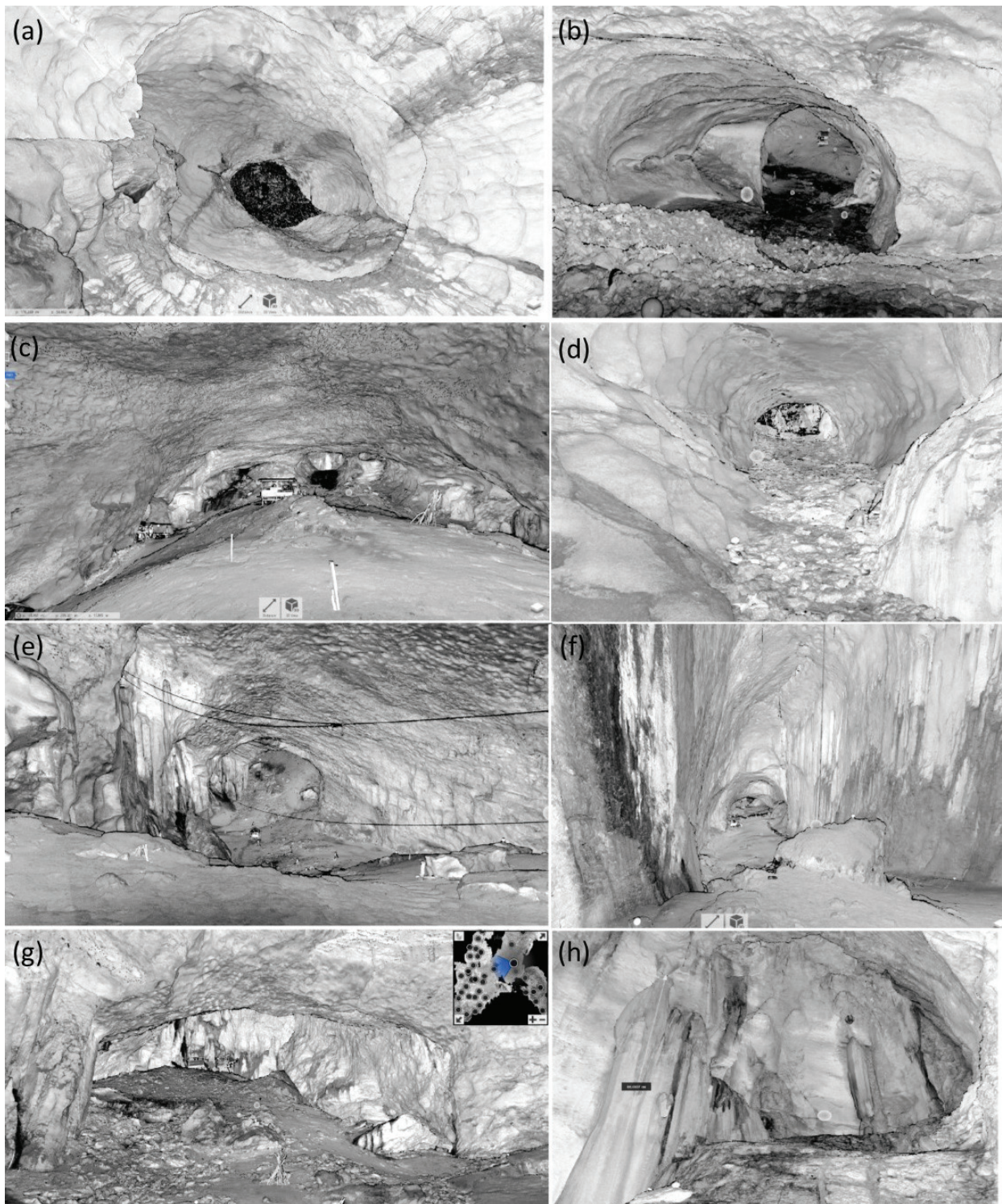


Figure 6. Intensity-based texture model of Simud Putih—topmost plate shows (a) the main entrance viewed from the base of the collapse sinkhole and (b) E-W direction towards the hall; plate (c) is the chamber viewed W-E, (d) shaft 1 viewing the entrance from inside, (e) main hall viewed to the southern end, (f) shaft 2 viewed northward; plate (g) views shaft 3 from the hall where the passage opens to it while (h) shows a section within shaft 3.

tube is preserved. The rate of passage modification seems to be at slow pace in the older passages. For example, within the chamber and main hall, scar of recent deformation can be found. Tonner variation distinguishes recently developed surfaces from the older ones. It can

be observed that the inner section of the entry passage, main hall, chamber and shaft 3 cavern belongs to the old formations. The old formations are discernible with much stable appearance, particularly at the roof which appears to form the base of harder rock strata. Those parts of the cave are favourable roosting locations for swiftlet birds in large numbers. Interestingly, bats and swiftlet birds can be differentiated from the texture model.

It is very clear that the development of the cave started from inside and, over time, eroded to the surface to provide entrances (see **Figure 6a** and **6d**). Similar imminent contact with surface is observed in shaft 3 which currently provides daylight openings along fractured zones that extend to about 118 m in length at the roof. The fault joins series of rock discontinuities (fault and fracture on the wall) that extend to the cave floor (see **Figure 7a** and **7c**). The roof around the daylight opening may eventually become collapse doline.

The floor of the cave is made up of fine mud sediments, rock debris, rock piles, plastic bottles, dendritic sediments, plates and polythene bags washed into the cave or abandoned by cavers. In the more weathered passages, a pile of rocks that broke away from the cave roof can be found on the floor. A stream of pebbles can be seen at the base of the sinkhole that form the entrance and also along shaft 1 passage which are transported into the cave and deposited along the passage floor. The occurrence of the cave passages and the pattern of post-speleogenetic decay have been largely influenced by the deformation characteristics of the rock rather than biogenic modifications because no perforated cave walls are observed in Simud Hitam.

Apart from shaft 3, the cave walls are solidly intact (**Figure 6**). Few base undercuts and wall notches are present at lower end of each passage where the eroded rocks have direct contact with the wall. Further, vestiges of fluted bay can be seen in shaft 3 though not as pronounced as those found in Simud Hitam. Other interesting wall morphologies include semi-circular pillar, cliff and hanging wall (**Figure 7b** and **7d**). A number of semi-circular pillars of varying diameters were identified on the wall of shaft 3. These pillars are made up of accumulated calcites dissolved in dripping waters from the cave roof. Evidence of this can be seen in the evolving shining glossy formations like stalactite (STT) and stalagmite (STM) approaching each other to form an unbroken pillar. All the pillars extend from the roof to the cave floor, measuring up to 20 m in height. We also identified other features such as cliffs and hanging walls (**Figure 7b**) within shafts 2 and 3. These features are certainly remnants of collapse blocks that are resistant weathering.

Generally, no lace-like or overtly perforated ceiling surface was observed; swiftlets take advantage of rock discontinuities within the more secured sections of the cave as niches to roost. The common morphological features identified in the cave roof include scallops, bell holes, ceiling pockets, roof avens, ceiling flush dome, seepage and hanging rocks (**Figure 8**). Except for the last three, the origin and development of these features have been well discussed in the literature [29, 30]. Scallops are predominantly retained in the more recently developed younger surfaces while traces of it are apparent in the older hard rock surfaces, but roof avens are common to weak rock surfaces. On the other hand, ceiling and conch pockets and bell holes are conventional outcomes of passive weathering on the older surfaces (chamber, hall, shaft 3 corridor and entry passages).

Ceiling flush dome is similar to semi-spherical flush mounted ceiling light, but unlike the bell-hole, the base flushes with the cave roof measuring between 20 and 80 cm in diameter,

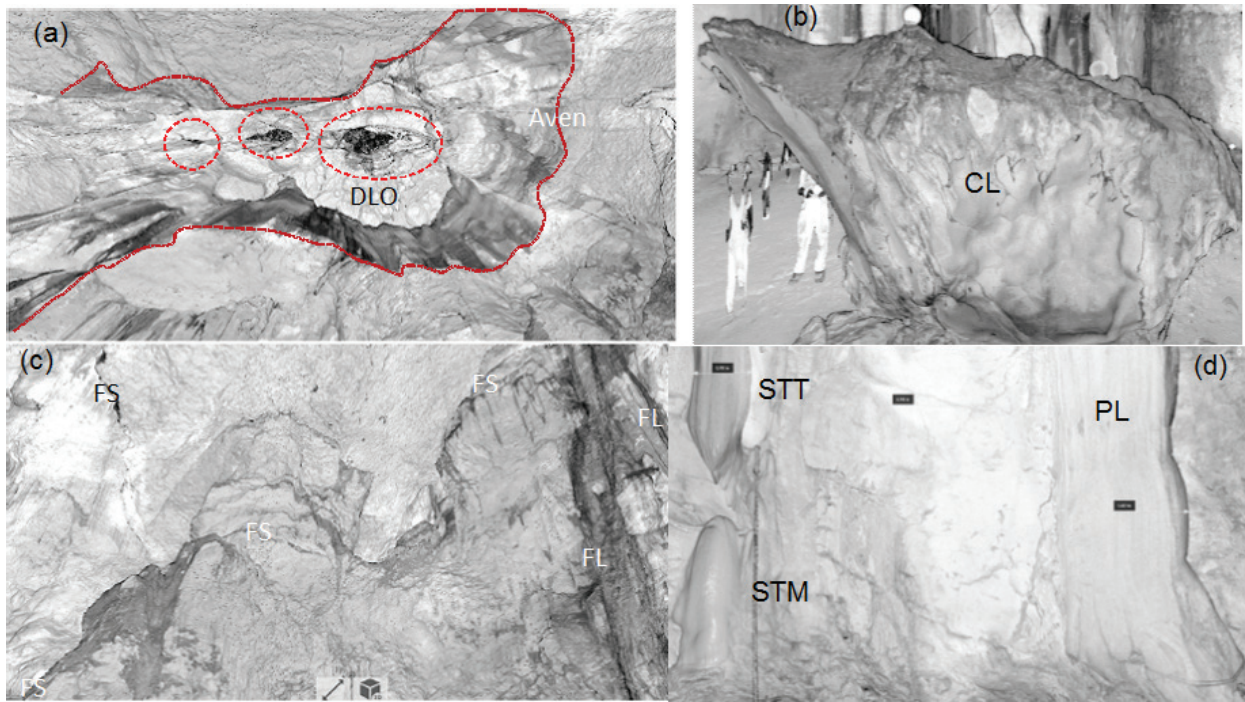


Figure 7. Rock surfaces: (a) daylight opening in the roof, (b) cliff, (c) fault and fractured wall and (d) semi-circular wall pillar (PL), including stalactite and stalagmite.

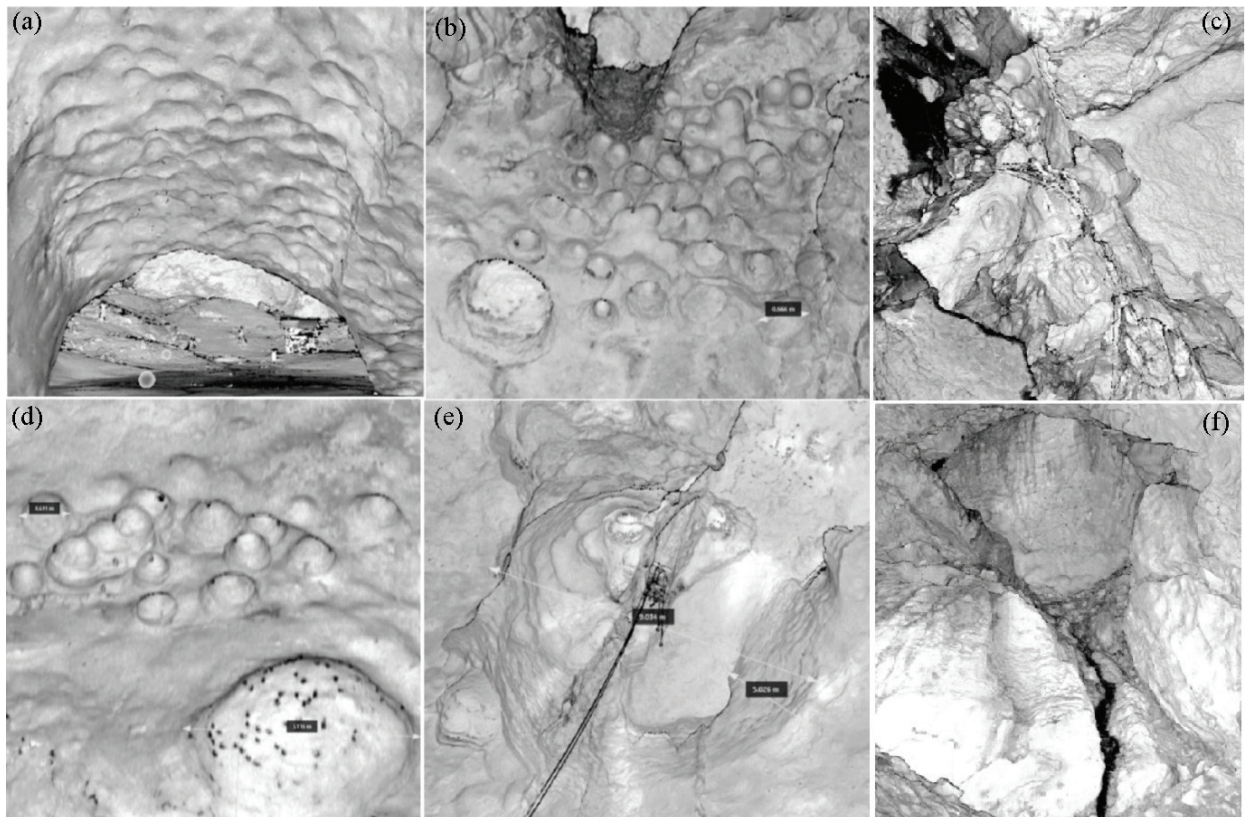


Figure 8. Cave roof morphologies: (a) scallops, (b) ceiling flush dome, (c) hanging rocks and fractures, (d) ceiling pockets and bell-hole, (e) ceiling aven of about 9 m in diameter and 5 m deep into the roof and (f) seepage.

suspended 30 cm from it. This particular roof feature is found in shaft 3. The feature may have originated from accumulation of calcite dissolved by water infiltration through carbonate rock. Another feature identified on the roof is the mass of rocks hanging on the roof, we call this hanging rock. This feature exists within unfavourable discontinuities especially where such fractures form follicular dendritic network that partitions weak rocks into loosely fragmented components. If the fracture reaches the surface, water may penetrate into the cave to create seepage. Seepage is a catalyst to cave deformation because it weakens the rock and speeds up the rate of weathering. A number of these features were identified in the roof and wall of the cave at different locations. Identification of seepage is important because it can help in predicting direction of future passage development and potential inlets.

4.4. Cave art visualization

Lack of efficient tools to combine geometric data and images has long made the process of producing virtual reality models from 3D scanning and texture information a difficult exercise. But with the emergence of new sensors and processing tools, the time and efforts needed to generate this product have been efficiently optimized, and the result obtained is so accurate that objects of sub-millimetre dimension can be detected and measured. As evidenced from virtual tour of the cave, people have been registering their presence in the cave by penning down ideas in written inscriptions and rock carvings over the years by striking directly on the rock surface (**Figure 9**).

One of the significances of the study is the demonstration of the ability of the high-resolution 3D texture model to detect carved rock and paintings on the wall and roof of the cave at sub-millimetre resolution. This result is novel and provides potential economic opportunities through tourism if well harnessed. A collection of archaeological treasures including pictographs, petroglyphs and inscriptions is found on the walls of the cave passages. The age of these engravings is not known, and no record is given about them. So, we believe they have no link with medieval traditional, spiritual or cultural use. It can be seen that some of the carvings are undergoing surface erosion and deterioration, and such can be quantitatively measured from the digital model. Identified litters in the floor of the cave are also bottles, plastics and disposable serving plates that are products of modern-day industries.

Exploiting the full potentials of this approach may play a significant role in geo-archaeological studies in the near future. Particularly, with the increasing availability of new high-quality digital sensors for data collection and efficient tools for data processing and analysis, qualitative recording, documentation and assessment of cave art are within the reach of archaeologists. The principal limiting factors to the adoption of this approach are the costs of acquiring the equipment and the considerable time and efforts required to train the users. While the added value to 3D documentation might not justify the investment, the multifunctional value of the data collected is far-reaching. A case in point is the increasing multidisciplinary perspective of cave research that has brought closer cooperation among archaeologists, geomatic engineers, geologists and other non-technical professionals [2]. This type of collaboration is required to offset cost implications through shared responsibilities without compromising precise documentation that yields better results.

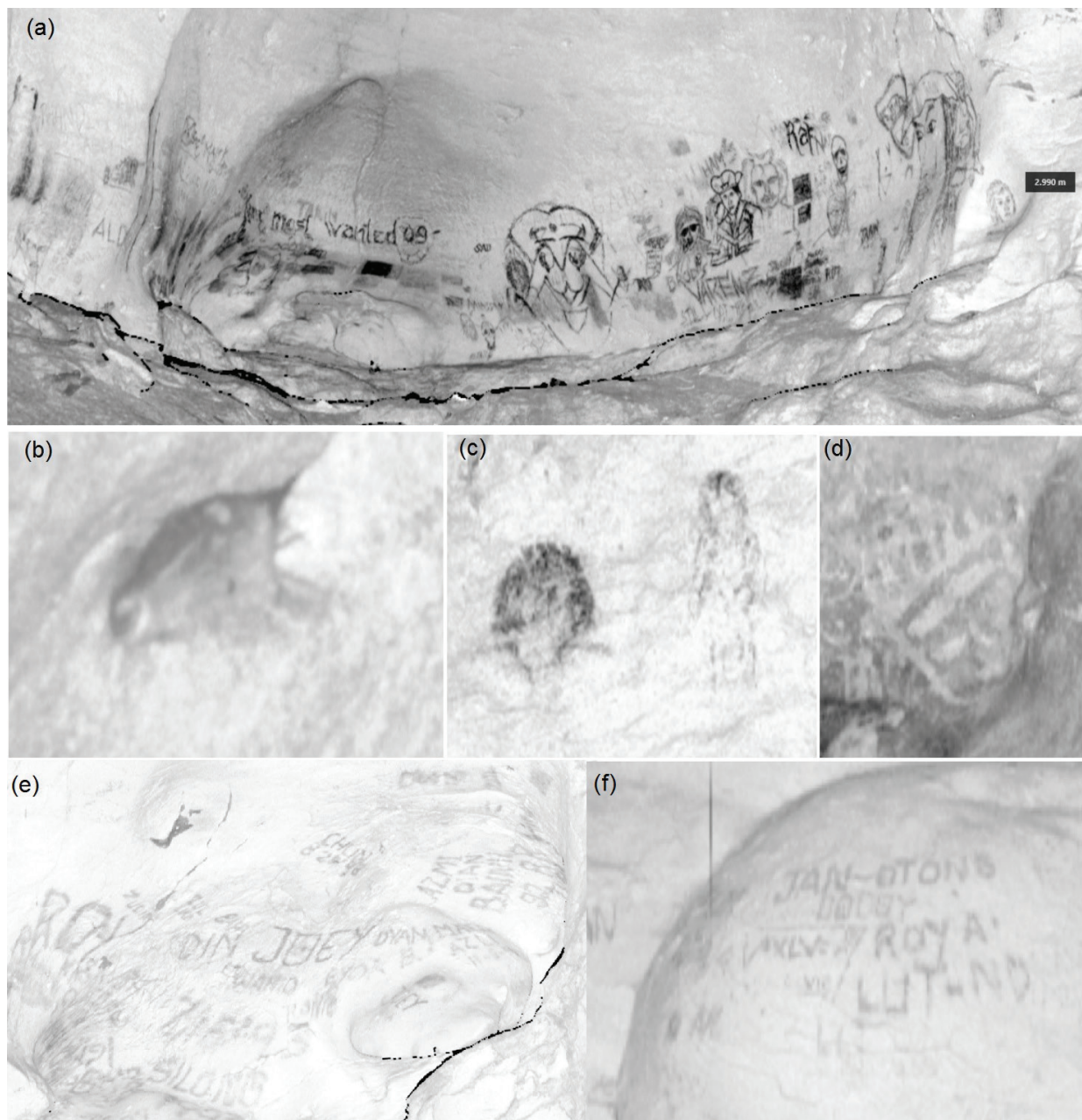


Figure 9. Cave arts on the wall—(a) paintings in shaft 1 (b, c), a picture of a goat head, and painting in shaft 3 and (d) cave engravings in the chamber and (e, f) cave inscriptions in entry passage.

5. Conclusion

Experience from this experimental work with intensity-based 3D texture model indicates a promising future for refined exploration of cave interiors at exceptionally high level of accuracy and details in areas that would challenge even the most adventurous caver. It is a paradigm shift from the era in which darkness in cave was seen as a major obstacle to visualization and information extraction. Given the versatility of laser-scanning data as demonstrated in this chapter, it is plausible to submit that further research will be required to adequately harness

the invaluable information therein embedded. This we believe is necessary to enhance further cave research and development. It is expected that as processing capabilities improve along with powerful sensor development, more applications are expected to emerge. The design of powerful modelling packages like ReCap 360 which performs parallel computing for 3D modelling and texturing bypasses the usually time-consuming matching of laser scans and photos and the associated manual editing. Similarly, increasing availability of other third-party point cloud oriented application software (open source and commercial) is broadening the sphere of possibilities with laser-scanning data. This development would change the phase of cave investigation across the different professional interest groups.

In terms of details, the full-scan model offers incredible clarity; objects as small as giant spiders and millipedes can be detected and measured. This is why it was evaluated for archaeological documentation. In the future, transmission of this information on the web can multiply its values and enhance knowledge sharing across platforms and agencies. The limitation of this approach is that it has no spatial analysis capability. Again, the problem of poor illumination still persists with natural RGB colour images, although it has little to do with geomorphological and geological applications such as those presented in this chapter.

Acknowledgements

This research is supported by Ministry of Higher Education, Malaysia research grant (FRGS/1-2014- STWN06/UPM//02/1) with vote number 5524502 and University Putra Malaysia research grant (GP- 1/2014/943200). The authors like to thank Professor Dr Manfred Buchroithner for joint terrestrial laser-scanning expedition funded by the National Geographic Society.

Author details

Mohammed Oludare Idrees and Biswajeet Pradhan*

*Address all correspondence to: biswajeet24@gmail.com

Department of Civil Engineering, Geospatial Information Science Research Center (GISRC), Faculty of Engineering, Universiti Putra Malaysia, Selangor Darul Ehsan, Malaysia

References

- [1] Tolan-Smite C. Human occupation of caves. In: Encyclopedia of Caves and Karst Science. Taylor and Francis Group, New York; 2004. pp. 919-924
- [2] Burens A, Grussenmeyer P, Guillemin S, Carozza L, Lévêque F, Mathé V. Methodological developments in 3D scanning and modelling of archaeological French heritage site: The Bronze Age painted cave of "Les Fraux", Dordogne (France). International Archives

- of the Photogrammetry, Remote Sensing and Spatial Information Sciences. 2013;**XL-5/W2**(131-135):2-6
- [3] Price L. Species diversity and food-web complexity in the caves of Malaysia. *Ambient Science*. 2014;**1**(2):1-8
- [4] Idrees MO, Pradhan B, Buchroithner MF, Shafri HZM, Bejo SK. Assessing the transferability of a hybrid Taguchi-objective function method to optimize image segmentation for detecting and counting cave roosting birds using terrestrial laser scanning data. *Journal of Applied Remote Sensing*. 2016;**10**(3):1-16
- [5] Gallay M, Hochmuth Z, Kaňuk J, Hofierka J. Geomorphometric analysis of cave ceiling channels mapped with 3D terrestrial laser scanning. *Hydrology and Earth System Sciences*. 2016;**2016**(February):1-48
- [6] Idrees MO, Pradhan B. A decade of modern cave surveying with terrestrial laser scanning: A review of sensors, method and application development. *International Journal of Speleology*. 2016;**45**(1):71-88
- [7] Lundberg J, McFarlane DA. Post-speleogenetic biogenic modification of Gomantong Caves, Sabah, Borneo. *Geomorphology*. 2012;**157-158**:153-168
- [8] Hutchison ES. *Geology of North West Borneo: Sarawak, Brunei and Saba*. Elsevier, Amsterdam; Boston 2005
- [9] Noad J. The Gomantong Limestone of Eastern Borneo: A sedimentological comparison with the near-contemporaneous Luconia Province. *Palaeo*. 2001;**175**(2001):273-302
- [10] Mcfarlane DA, Buchroithner M, Lundberg J, Petters C, Roberts W, Van Rentergen G. Integrated three-dimensional laser scanning and autonomous drone surface-photogrammetry at Gomantong Caves, Sabah, Malaysia. In: 2013 ICS Proceedings: Karst and Cave Survey, Mapping and Data Processing—Poster, Czech Speleological Society, Czech Republic, Brno 2013. pp. 317-319
- [11] Kingston T. Research priorities for bat conservation in Southeast Asia: A consensus approach. *Biodiversity and Conservation*. 2010;**19**(2):471-484
- [12] Abdullah MT, Paul IV, Hall L. A frightful stairway to cave bats in Borneo. *Bat Conservation International*. 2005;**23**(3):11-13
- [13] Lim KH, Khoo CK, Laurentius NA, Yeo BK. A preliminary report on the surveillance of Highly Pathogenic Avian Influenza (H5N1) and Newcastle Disease (ND) viruses in edible bird nest swiftlet (*Aerodramus fuciphagus* and *Aerodramus maximus*). *Malaysian Journal of Veterinary Research*. 2012;**3**(1):1-5
- [14] McFarlane D, Roberts W, Buchroithner M, Van Rentergem G, Lundberg J, Hautz S. Terrestrial LiDAR-based automated counting of swiftlet nests in the caves of Gomantong, Sabah, Borneo. *International Journal of Speleology*. 2015;**44**(2):55-60

- [15] Dublyansky Y, Roncat A, Spötl C, Dorninher P. Hypogene cave morphology at high resolution: Full 3-D survey of Märchenhöhle (Austria). In: Chavez T, Reehling P, editors. *Proceeding of Deepkarst 2016: Origins, Resources, and Management of Hypogene Karst*; 11-14 April; Carlsbad, New Mexico, USA: National Cave and Karst Research Institute; 2016. pp. 183-187
- [16] Chandelier L, Roche F. Terrestrial laser scanning for paleontologists: The Tautavel Cave. In: *XXII CIPA Symposium: Digital Documentation, Interpretation & Presentation of Cultural Heritage*; 11-15 October 2009; Kyoto, Japan. ICOMOS, Paris, France. 2009. pp. 1-5
- [17] Tsakiri M, Sigizis K, Billiris H, Dogouris S. 3D laser scanning for the documentation of cave environments. In: *11th ACUUS Conference: Underground Space, Expanding the Frontiers*; 10-13 September 2007; Athens, Greece. ACUUS, Greece. 2007. pp. 403-408
- [18] Besl P, McKay N. A method for registration of 3-D shapes. *IEEE Transactions on Pattern Analysis and Machine Intelligence*. 1992;**14**(2):239-256
- [19] Huber D. The ASTM E57 file format for 3D imaging data exchange. In: *Proceedings of the SPIE Vol. 7864A, Electron Imaging Science and Technology Conference (IS&T), 3D Imaging Metrology*, SPIE, USA. 2011. pp. 1-9
- [20] CloudCompareV2.8. GPL Software [Internet]. 2016. Available from: <http://www.cloud-compare.org/>. [Accessed: 15 August 2016]
- [21] Cignoni P, Ranzuglia G. MeshLab. Visual Computing Lab [Internet]. ISTI-CNR. 2014. Available from: <http://meshlab.sourceforge.net/>. [Accessed: 26 December 2016]
- [22] Silvestre I, Rodrigues JI, Figueiredo MJG, Veiga-Pires C. Cave chamber data modeling and 3D web visualization. In: *Proceeding of International Conference Information Visualisation*, IEEE Computer Society, USA. 2013. pp. 468-473
- [23] Silvestre I, Figueiredo M, Veiga-pires C. High-resolution digital 3D models of Algar do Penico Chamber: Limitations, challenges, and potential. *International Journal of Speleology*. 2015;**44**(January):25-35
- [24] Lerma JL, Navarro S, Cabrelles M, Villaverde V. Terrestrial laser scanning and close range photogrammetry for 3D archaeological documentation: The Upper Palaeolithic Cave of Parpalló as a case study. *Journal of Archaeological Science*. 2010;**37**:499-507
- [25] González-Aguilera D, Muñoz-Nieto A, Gómez-Lahoz J, Herrero-Pascual J, Gutierrez-Alonso G. 3D digital surveying and modelling of cave geometry: Application to Paleolithic rock art. *Sensors*. 2009;**9**(1):1108-1127
- [26] Gonzalez-Aguilera D, Rodriguez-Gonzalvez P, Mancera-Taboada J, Muñoz-Nieto A, Herrero-Pascual J, Gomez-Lahoz J. Application of non-destructive techniques to the recording and modelling of Palaeolithic rock art. In: Wang C-C, editor. *Laser Scanning, Theory and Applications*. InTech; Open Science Publisher. 2011. pp. 305-326

- [27] El-Hakim SF, Fryer J, Picard M. Modeling and visualization of Aboriginal rock art in the Baiame Cave. In: Proceeding of XXth Congress of the International Society for Photogrammetry and Remote Sensing; 12-23 July 2004; Istanbul, Turkey: Comm V, Work Gr V/2; 2004. pp. 990-995
- [28] Autodesk. Autodesk Software for Students, Educators, and Educational Institutions [Internet]. Autodesk Education Community. 2017. Available from: <http://www.autodesk.com/education/free-software/featured>. [Accessed: 4 November 2016]
- [29] Lacanette D, Large D, Ferrier C, Aujoulat N, Bastian F, Denis A, et al. A laboratory cave for the study of wall degradation in rock art caves: An implementation in the Vezere area. *Journal of Archaeological Science*. 2013;**40**(2):894-903
- [30] Plan L, Tschegg C, De Waele J, Spötl C. Corrosion morphology and cave wall alteration in an Alpine sulfuric acid cave (Kraushöhle, Austria). *Geomorphology*. 2012;**169-170**:45-54